Non-local Field Effects in Nonlinear Plasmonic Metasurfaces

Mikko J. Huttunen[1], Saad Bin-Alam[2], Orad Reshef[3], Y. Mamchur[2,4], Timo Stolt[1], Jean-Michel Ménard[3], Ksenia Dolgaleva[2,3], Robert W. Boyd[2,3,5], and Martti Kauranen[1]

[1]*Photonics Laboratory, Physics Unit, Tampere University, Tampere, Finland*
[2]*School of Electrical Engineering and Computer Science, University of Ottawa, Ottawa, ON K1N 6N5, Canada*
[3]*Department of Physics, University of Ottawa, Ottawa, ON K1N 6N5, Canada*
[4]*National Technical University of Ukraine "Igor Sikorsky Kyiv Polytechnic Institute," Kyiv, Ukraine*
[5]*The Institute of Optics and Department of Physics and Astronomy, University of Rochester, Rochester, New York 14627, USA*
Tel: (35850) 4921272, e-mail: mikko.huttunen@tuni.fi

ABSTRACT
Nonlinear optical processes are important in many photonic applications ranging from optical communications and ultrashort pulse generation to frequency combs. Recent trend to miniaturize photonic components has created a growing demand also for nanoscale nonlinear components. This demand is difficult to answer by using conventional nonlinear materials motivating the search for alternatives. Nonlinear plasmonic metasurface cavities have recently emerged as a potential platform to enable nanoscale nonlinear optics. Despite steady progress, the so far achieved conversion efficiencies have not yet rivalled conventional materials. Here, we present our recent work to develop more efficient nonlinear metamaterials, focusing on plasmonic metasurfaces that support collective responses known as surface lattice resonances. These resonances are associated with very narrow spectral features, showing potential to dramatically boost nonlinear processes via resonant interactions. Here, we demonstrate a plasmonic metasurface operating at the telecommunications C band that exhibits a record-high quality factor exceeding 2000, demonstrating an order-of-magnitude improvement compared to existing metasurface cavities. Motivated by this experimental demonstration, we will also present numerical predictions suggesting that such nonlinear metasurfaces could soon answer the existing demand for miniaturized and/or flat nonlinear components.
Keywords: Nonlinear optics, metasurfaces, plasmonics, frequency conversion, resonators, plasmonics.

1. INTRODUCTION

An optical cavity is a component that stores light oscillating at the resonant frequency of the cavity. Such components are crucial in many fields of photonics ranging from sensing and laser development to nonlinear optics [1]. Traditionally, optical cavities have consisted of two facing mirrors. However, recently, waveguide-based cavities such as whispering gallery mode resonators, microring resonators and photonic crystal cavities have gained popularity [2–5]. Despite the very high quality factors (Q-factors) of these very small footprint devices, their operation is not always without problems. For example, it is often difficult to efficiently couple a free-space propagating beam of light into these devices.

It has been recently realized that periodic arrays of nanoparticles, also known as metasurfaces, can also act as optical cavities [6]. Interestingly, a metasurface cavity can be easily accessed by using a free propagating beam, and operates entirely within a sub-wavelength propagation region, i.e, is essentially a flat component. Because of these advantages over waveguide-based cavities, a metasurface cavity platform could potentially find use in many photonic applications. The main challenge in realized metasurface cavities has so far been their poor cavity lifetimes hindering their use in potential applications. For example, the resonances associated with individual plasmonic nanoparticles known as localized surface plasmon resonances (LSPRs) are associated with low Q-factors ($Q < 10$). An order of magnitude improvement in achieved Q-factors ($Q \sim 100$) has been recently demonstrated by utilizing dielectric nanoparticle resonators [7, 8]. Interestingly, it has been suggested that dramatically higher Q-factors could be achieved by utilizing collective responses occurring in metasurfaces [9, 10]. These collective responses, known as surface lattice resonances (SLRs), have already been utilized, for example, to demonstrate plasmonic lasers and enhanced nonlinear optical interactions [11–15]. However, their experimentally demonstrated Q-factors have been so far limited to few hundreds.

Here, we demonstrate a plasmonic metasurface cavity design that supports an ultra-high-Q SLR ($Q \approx 2400$) at $\lambda = 1545$ nm [16]. Motivated by this experimental demonstration, we will also use nonlinear discrete-dipole approximation (NDDA) to perform numerical simulations of second-harmonic generation (SHG) from such high-Q metasurfaces [17]. Over million-fold SHG intensity enhancements are predicted suggesting that nonlinear metasurfaces could soon answer the existing demand for miniaturized and flat nonlinear components.

2. HIGH-Q PLASMONIC METASURFACES

In order to understand the formation of high-Q SLRs, we introduce a semi-analytical model known as the lattice sum approach (LSA) [9, 18, 19]. The optical response of a single nanoparticle can be described by using the particle polarizability α which connects the incident field E to the dipole moment of the particle p via $p = \varepsilon_0 \alpha E$, where ε_0 is the vacuum permittivity. The α is often taken to be a simple Lorentzian profile

$$\alpha_{\text{lor}} = \frac{A_0}{(\omega - \omega_0) + i\gamma}, \tag{1}$$

where the amplitude A_0 represents the oscillator strength, ω_0 corresponds to the nanoparticle resonance frequency, and γ is the damping term. In order to describe the optical responses of nanoparticles accurately also further away from the LSPR, we use of the so-called modified long wavelength approximation and take α to be [20, 21]

$$\alpha(\omega) = \frac{\alpha_{\text{lor}}(\omega)}{1 - \frac{2}{3} ik^3 \alpha_{\text{lor}}(\omega) - \frac{k^2}{l} \alpha_{\text{lor}}(\omega)}, \tag{2}$$

where l is the effective length of the particle and $k = 2\pi/\lambda$ is the wavenumber. In general, the particle polarizability depends on the particle geometry and material.

The contribution of the surrounding nanoparticles, i.e. the lattice, to the polarizability α can be taken into account by introducing an effective polarizability [18]

$$\alpha^* = \frac{\alpha}{1 - \varepsilon_0 \alpha S} = \frac{1}{1/\alpha - \varepsilon_0 S}, \tag{3}$$

where S is the lattice sum that depends on the lattice arrangement [9]. Looking at Eq. (3) we see that an SLR appears if the imaginary part of α^* peaks near wavelength of $\omega_{SLR} = 2\pi c/\lambda_{SLR}$. We describe the transmission T of the metasurface as

$$T = 1 - \frac{4\pi k}{p_x p_y} \Im(\alpha^*), \tag{4}$$

where p_i are the lattice periods (along x and y directions). We see that by choosing proper nanoparticle dimensions and a metasurface lattice geometry, a high-Q metasurface can be designed [9].

Here, such a high-Q metasurface was designed by arranging rectangular gold nanobars (lengths $L_y = 200$ nm, widths $L_x = 130$ nm and heights $t = 20$ nm) into a rectangular array with periodicities of $p_x = 500$ nm and $p_y = 1060$ nm, immersed in a homogeneous environment with refractive index of $n = 1.45$ (see Fig. 1a). The area of the fabricated metasurface was $600 \times 600\,\mu\text{m}^2$, consisting therefore of around 1200×567 particles. Based on finite-difference time domain (FDTD) simulations this metasurface was expected to support a LSPR near 850 nm and a high-Q SLR near 1550 nm. Performed LSA calculations verify this prediction and are shown in Figs. 1b–c, for an x-polarized beam incident at normal incidence. The measured transmission spectra are shown in Figs. 1b–c, matching well the calculated spectra. Notably, the full width at half-maximum of the linewidth of the SLR is only $\Delta\lambda = 0.66$ nm, corresponding to a record-high quality factor of $Q = 2400$.

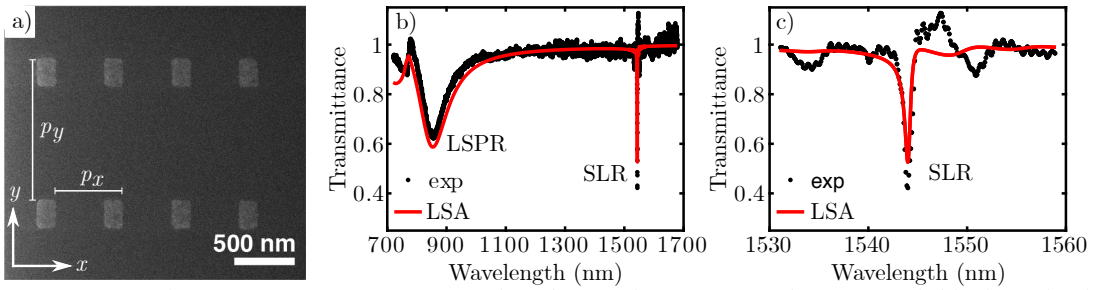

Figure 1. a) Helium-ion microscope image of the fabricated metasurface. b) Measured (black) and calculated (red) transmission spectra showing the LSPR (850 nm) and SLR (1535 nm). c) High-resolution plot of the SLR exhibiting an ultra-narrow linewidth of 0.66 nm, corresponding to $Q \approx 2400$.

3. MULTIRESONANT NONLINEAR METASURFACES

Next, we generalize the above LSA to nonlinear responses and finite arrays [17, 22], being primarily motivated to investigate metasurface designs that could support multiple high-Q SLRs. By designing such metasurfaces to exhibit high-Q resonances, not just near the fundamental pump frequency, but also near the signal frequencies of interest, multiresonant nonlinear structures could be realized [19, 23]. Following the approach outlined in Refs. [13, 17, 22], we write the effective hyperpolarizability corresponding to the process of SHG as

$$\beta^*(2\omega;\omega,\omega) = \frac{\beta(2\omega;\omega,\omega)}{[1 - \varepsilon_0 \alpha(2\omega) S(2\omega)]\,[1 - \varepsilon_0 \alpha(\omega) S(\omega)]^2}, \tag{5}$$

where $\beta(2\omega;\omega,\omega)$ is the hyperpolarizability of a single nanoparticle, and ω and 2ω correspond to fundamental and SHG frequencies, respectively. A reader interested in other nonlinear processes is adviced to look into Refs. [13, 22]. Looking at Eq. (5) we see that by careful design of the nanoparticle and lattice parameters, the effective hyperpolarizability β^* can be made to exhibit two sharp SLRs at the two frequencies of interest (here at ω and 2ω). The extension of the above approach to finite arrays and arbitrary excitation field profiles is done by using nonlinear discrete-dipole approximation (NDDA), which takes explicitly into account the scattered fields from every particle in the metasurface [17, 24]. In essence, using NDDA we solve numerically the scattering problem for N nanoparticles by transforming the problem into a system of $3N$ linear equations, which is then solved via matrix inversion methods [25].

Here, we introduce a metasurface design consisting of asymmetric L-shaped aluminum nanoparticles with thicknesses $h = 30$ nm, left-side arm length $l_1 = 100$ nm, right-side arm length $l_2 = 90$ nm and arm width $w = 45$ nm (Fig. 2a). Although gold is a typical plasmonic material, we were not able to find particle dimensions that would have supported LSPRs at wavelengths considerably shorter than the designed SHG wavelength (near 600 nm). Because this design criteria is important for formation of high-Q SLRs, gold was found to be an unsuitable material. Subsequently, the nanoparticles were chosen to be made from aluminum which allowed the shorter wavelength LSPR to peak near 470 nm, supporting emergence of high-Q SLRs at longer wavelengths [17]. The nanoparticles were arranged into a rectangular lattice with the periods $p_x = 395$ nm and $p_y = 793$ nm, giving rise to the two high-Q SLRs at the second-harmonic (600 nm) and the fundamental wavelengths (1200 nm), respectively (Fig. 2b). The simulated metasurface consisted of 600×600 particles corresponding to a physical size of around $250 \times 500\,\mu\text{m}^2$.

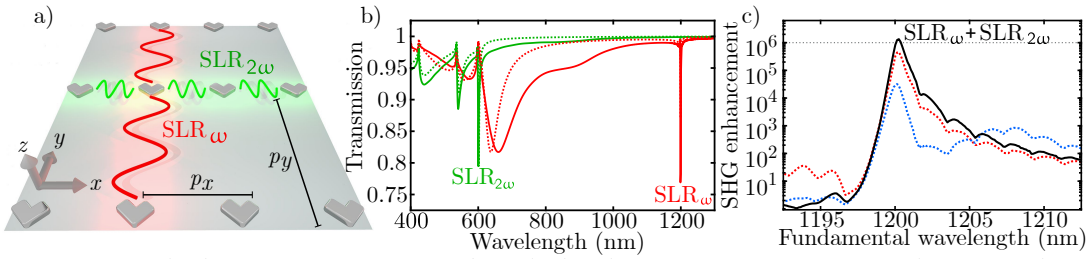

Figure 2. a) Multiply-resonant metasurface. b) Calculated transmission spectra using the NDDA (dotted lines) and the FDTD (solid lines). Red (green) curves correspond to x-polarized (y-polarized) incident light. c) Predicted SHG intensity enhancement for a particle at the center of the metasurface. 1 389 200-fold enhancement occurs for the doubly-resonant metasurface (black solid line). Varying p_x the SHG emission decreases (red and blue dotted lines).

We calculated the transmission spectra of the designed multiresonant metasurface (see Fig. 2b) using both the FDTD (solid lines) and the NDDA (dotted lines). The shorter wavelength LSPR associated with the L-shaped nanostructures was excited using normally incident y-polarized light and resulted in an SLR near 600 nm (green lines). The associated Q-factor of this SLR (SLR$_{2\omega}$) was calculated to be 250. The longer wavelength LSPR associated with the L-shaped nanostructures was excited using normally incident x-polarized light and resulted in an SLR near 1200 nm (red lines). The associated Q-factor of this SLR (SLR$_{\omega}$) was calculated to be 800.

SHG emission intensity enhancement for a single particle at the center of the metasurface was calculated using the NDDA [17]. Notably, over a million-fold intensity enhancement of SHG emission was predicted to occur when the fundamental and SHG frequencies coincided spectrally with the SLRs (Fig. 2c). In order to verify that the enhancement was of doubly-resonant origin, the SHG simulations were repeated for slightly varied periods p_x. Mainly, variations in p_x shift the SLR$_{2\omega}$ and make the metasurface singly resonant. The slight detuning of the period from the value $p_x = 395$ nm to 393 nm and 398 nm resulted in an over order of magnitude decrease in the overall SHG enhancement near 1200 nm (see the red and blue dotted lines in Fig. 2c, respectively). Particularly, the predicted SHG enhancement factors were found to be 465 900 and 31 600 for $p_x =$ 393 nm and 398 nm, respectively. By looking at these values it is therefore clear, that majority of the predicted resonance enhancement for the doubly-resonant metasurface is due to the resonance enhancement at the fundamental wavelength. This is expected because the SHG process depends quadratically on the fundamental field strength. These results verified the doubly-resonant origin of the original SHG enhancement using $p_x = 395$ nm.

4. CONCLUSION

We have demonstrated an SLR-based plasmonic metasurface nanocavity with a record-high Q-factor (here 2400). We believe that such high-Q metasurfaces will dramatically expand the capabilities of metasurfaces for many optical applications. We have also numerically demonstrated an approach to realize multiresonant metasurfaces, which

could enable applications benefiting of multiple high-Q resonances. In particular, we believe that such multiresonant high-Q metasurfaces could be useful for nonlinear optical applications such as for frequency conversion, photon-pair creation or terahertz-wave generation.

ACKNOWLEDGEMENTS

We acknowledge the support of the Academy of Finland (Grant No. 308596) and the Flagship of Photonics Research and Innovation (PREIN) funded by the Academy of Finland (Grant No. 320165).

REFERENCES

1. K. J. Vahala, "Optical microcavities," *Nature*, vol. 424, pp. 839–846, 2005.
2. X. Zhang, H. S. Choi, and A. M. Armani, "Ultimate quality factor of silica microtoroid resonant cavities," *Appl. Phys. Lett.* vol. 96, p. 153304, 2010.
3. X. Ji et al., "Ultra-low-loss on-chip resonators with sub-milliwatt parametric oscillation threshold," *Optica*, vol. 4, pp. 619–624, 2017.
4. T. Asano et al., "Photonic crystal nanocavity with a Q factor exceeding eleven million," *Opt. Express*, vol. 25, pp. 1769–1777, 2017.
5. C. W. Hsu et al., "Observation of trapped light within the radiation continuum," *Nature*, vol. 499, pp. 188–191, 2013.
6. N. Meinzer, W. L. Barnes, and I. R. Hooper, "Plasmonic meta-atoms and metasurfaces," *Nat. Photonics*, vol. 8, pp. 889–898, 2014.
7. L. Carletti et al., "Giant Nonlinear Response at the Nanoscale Driven by Bound States in the Continuum," *Phys. Rev. Lett.* vol. 121, p. 33903, 2018.
8. K. Koshelev et al., "Subwavelength dielectric resonators for nonlinear nanophotonics," *Science (80-.).* vol. 367, pp. 288–292, 2020.
9. M. J. Huttunen et al., "Ultra-strong polarization dependence of surface lattice resonances with out-of-plane plasmon oscillations," *Opt. Express*, vol. 24, pp. 28279–28289, 2016.
10. V. G. Kravets et al., "Plasmonic Surface Lattice Resonances: A Review of Properties and Applications," *Chem. Rev.* vol. 118, pp. 5912–5951, 2018.
11. W. Zhou et al., "Lasing action in strongly coupled plasmonic nanocavity arrays," *Nat. Nanotechnol.* vol. 8, pp. 506–511, 2013.
12. T. K. Hakala et al., "Lasing in dark and bright modes of a finite-sized plasmonic lattice," *Nat. Commun.* vol. 8, p. 13687, 2017.
13. L. Michaeli et al., "Nonlinear Surface Lattice Resonance in Plasmonic Nanoparticle Arrays," *Phys. Rev. Lett.* vol. 118, p. 243904, 2017.
14. D. C. Hooper et al., "Second harmonic spectroscopy of surface lattice resonances," *Nano Lett.* vol. 19, pp. 165–172, 2018.
15. R. Czaplicki et al., "Less is more – enhancement of second-harmonic generation from metasurfaces by reduced nanoparticle density," *Nano Lett.* vol. 18, pp. 7709–7714, 2018.
16. M. S. Bin-Alam et al., "Ultra-high-Q resonances in plasmonic metasurfaces," *arXiv:2004.05202 [physics.optics]*, 2020.
17. M. J. Huttunen et al., "Efficient nonlinear metasurfaces by using multiresonant high-Q plasmonic arrays," *J. Opt. Soc. Am. B*, vol. 36, E30–E35, 2019.
18. V. A. Markel, "Coupled-dipole approach to scattering of light from a one-dimensional periodic dipole structure," *J. Mod. Opt.* vol. 40, pp. 2281–2291, 1993.
19. O. Reshef et al., "Multiresonant high-Q plasmonic metasurfaces," *Nano Lett.* vol. 19, pp. 6429–6434, 2019.
20. T. Jensen et al., "Electrodynamics of noble metal nanoparticles and nanoparticle clusters," *J. Clust. Sci.* vol. 10, pp. 295–317, 1999.
21. B. Auguié and W. L. Barnes, "Collective resonances in gold nanoparticle arrays," *Phys. Rev. Lett.* vol. 101, p. 143902, 2008.
22. M. J. Huttunen, R. Czaplicki, and M. Kauranen, "Nonlinear plasmonic metasurfaces," *J. Nonlinear Opt. Phys. Mater.* vol. 28, p. 1950001, 2019.
23. M. Celebrano et al., "Mode matching in multiresonant plasmonic nanoantennas for enhanced second harmonic generation," *Nat. Nanotechnol.* vol. 10, pp. 412–417, 2015.
24. M. J. Huttunen et al., "Using surface lattice resonances to engineer nonlinear optical processes in metal nanoparticle arrays," *Phys. Rev. A*, vol. 97, p. 053817, 2018.
25. B. T. Draine and P. J. Flatau, "Discrete-dipole approximation for scattering calculations," *J. Opt. Soc. Am. A*, vol. 11, 1994.